Back to Contents

High-Performance MoS_2 Field-Effect Transistors Enabled by Chloride Doping: Record Low Contact Resistance (0.5 kΩ·µm) and Record High Drain Current (460 µA/µm)

Lingming Yang[1], Kausik Majumdar[2*], Yuchen Du[1], Han Liu[1], Heng Wu[1], Michael Hatzistergos[3], P. Y. Hung[2], Robert Tieckelmann[2], Wilman Tsai[4], Chris Hobbs[2], and Peide D. Ye[1#]

[1]*School of Electrical and Computer Engineering, Purdue University, West Lafayette, IN 47906, U.S.A.*
[2]*SEMATECH, Albany, NY 12203, U.S.A.* [3]*SUNY CNSE, Albany NY 12203, U.S.A.* [4]*Intel Corporation, Santa Clara, CA 95054, U.S.A.*
Tel: 1-765-494-7611, Fax: 1-765-496-7443, E-mail: [#]yep@purdue.edu, [*]kausik.majumdar@sematech.org

Abstract

In this paper, we report a novel chemical doping technique to reduce the contact resistance (R_c) of transition metal dichalcogenides (TMDs) – eliminating two major roadblocks (namely, doping and high R_c) towards demonstration of high-performance TMDs field-effect transistors (FETs). By using 1,2 dichloroethane (DCE) as the doping reagent, we demonstrate an active n-type doping density > 2×10^{19} cm^{-3} in a few-layer MoS_2 film. This enabled us to reduce the R_c value to a record low number of 0.5 kΩ·µm, which is ~10× lower than the control sample without doping. The corresponding specific contact resistivity (ρ_c) is found to decrease by two orders of magnitude. With such low R_c, we demonstrate 100 nm channel length (L_{ch}) MoS_2 FET with a drain current (I_{ds}) of 460 µA/µm at V_{ds} = 1.6 V, which is twice the best value reported so far on MoS_2 FETs.

Introduction

Semiconducting TMDs possess unique electrical and optical properties due to their d-electron orbitals and 2D nature [1,2]. Among TMDs, MoS_2 has attracted the most attention for its potential applications in low-power electronics [3,4]. However, high R_c value limits the device performance of MoS_2 FETs significantly and the realization of ohmic contacts for MoS_2 remains a challenge so far [5]. There were several attempts to reduce R_c including use of low workfunction metal [6] and employing edge contact concept [7]. One of the keys to resolve this issue is to dope the MoS_2 film, however doping the atomically thin film is nontrivial and requires a simple and reliable process technique [8-10]. In this work, we demonstrate such a doping technique enabling high-performance MoS_2 FET.

Fabrication and Physical Characterization

Fig. 1(a) schematically shows the MoS_2 back-gate FET fabricated in this work. Few-layer MoS_2 flakes were mechanically exfoliated from bulk MoS_2 on a 90 nm SiO_2/p^{++} Si substrate and then soaked in DCE. Acetone and isopropanol rinses were used to remove the residue of the chemical. After e-beam lithography, Ni (30 nm)/Au (60 nm) were deposited to form S/D contacts. The thickness of the MoS_2 flake was identified by the optical image (Fig. 2(a)) and measured by the AFM (Fig. 2(b)). The flake thickness was ~4 nm, corresponding to about 6 monolayers. Fig. 2(c) shows an SEM image of a fabricated TLM structure. The presence of Cl in DCE treated MoS_2 film was confirmed by XPS and SIMS, as shown in Fig. 3 (a) and (b). In Fig. 4, we observe a relative blue shift in the binding energies of the core level peaks of the MoS_2 sample that was treated with DCE, which results from an upward shift in the Fermi level, and hence can be attributed to an n-type doping of the sample. However, we note that Cl, when acts as an adatom dopant, results in p-type doping in MoS_2 film [11]. Thus, such n-type doping can be attributed to the donation of extra electron when substitution of S^{2-} by Cl^- takes place, particularly at the sites of sulfur vacancies in the MoS_2 film.

Contact Resistance Reduction

The TLM resistances of MoS_2 FETs at 50 V back-gate-bias (V_{bg}) with and without the Cl doping are plotted as a function of contact separations in Fig. 5(a). The extracted R_c is significantly reduced from 5.4 kΩ·µm to 0.5 kΩ·µm after the Cl doping. Such an improvement in R_c is attributed to the doping induced thinning of tunneling barrier width. In Fig. 6, we observe that the extracted R_c is a weak function of temperature (although the sheet resistance changes by a factor of 2), indicating the dominance of tunneling component of the current over thermionic component at the contact interface. In order to determine the ρ_c, the transfer lengths (L_T) of Ni-MoS_2 junctions are extracted by the TLM and are determined to be 60 nm and 590 nm for the contacts with and without the Cl doping, respectively. Compared with the control sample without the Cl doping, the ρ_c is reduced from 3×10^{-5} Ω·cm^2 to 3×10^{-7} Ω·cm^2 when the DCE treatment time is 36 hours, as shown in Fig. 7. The n-type doping concentration (N_d) by chloride is ~2.3×10^{19} cm^{-3} extracted from the slope of the TLM fitting when V_{bg} is 0 V. Fig. 8 shows the channel resistance and the R_c as a function of V_{bg} for a 1 µm device. Usually in back-gated MoS_2 FETs, R_c strongly depends on V_{bg} because V_{bg} would electrostatically dope the semiconductor underneath the contact, thus reducing the R_c. In this work, the R_c shows very weak dependence on V_{bg} when V_{bg} is larger than -30 V, indicating heavily doped S/D regions are realized. Since back gate is not necessary for achieving the low R_c any more, it paves the way to realize three-terminal top-gate low-R_c MoS_2 FETs. The present Cl doping technique with DCE treatment is also valid for the other TMD materials such as WS_2, whose E_F is pinned near the middle of the band bandgap.

Electrical Performance of MoS_2 FET

Fig. 9 shows the output characteristics of 100 nm L_{ch} MoS_2 FETs with and without the Cl doping. The reduced R_c helps to boost the I_{ds} from ~ 110 µA/µm to 460 µA/µm at V_{ds} = 1.6 V, which is twice of the best reported value so far on MoS_2 FETs at the same L_{ch} [6]. Fig. 10 shows the components of total resistance (R_{total}) indicating mitigation of the adverse dominance of high Schottky S/D contact resistance (R_{sd}) at 100 nm L_{ch}. Such reduction in R_{sd} also results in excellent current saturation, as observed in Fig. 9. The transfer characteristics of the two devices are shown in Fig. 11. Due to its relatively large bandgap and ultra-thin channel, we achieved an excellent I_{on}/I_{off} of ~6.3×10^5. Considering the thick gate oxide (90 nm) used in this work, the I_{on}/I_{off} ratio can be further improved by EOT scaling down. As shown in Fig. 12, the intrinsic long channel field-effect motility (μ_{FE}) as a function of gate electric field is calculated for different L_{ch} by appropriately eliminating the R_{sd} effect with a peak μ_{FE} of 50-60 cm^2/Vs. Fig. 13 benchmarks the I_{ds} (V_{ds} = 1.6 V) and the R_c for MoS_2 FETs in literature [5-7, 12-13]. Due to the significant reduction of R_c, the present work shows superior performance at various L_{ch} compared with existing literature. These results indicate that the Cl doping by the DCE treatment is an effective way to realize low contact resistance MoS_2 FETs. Table 1 summarizes the electrical performance of the presented devices.

Conclusion

For the first time, a record low R_c of 0.5 kΩ·µm is achieved on the MoS_2 FET with Cl doping technique. As a result, the ρ_c significantly decreases from 3×10^{-5} Ω·cm^2 to 3×10^{-7} Ω·cm^2. The 100 nm L_{ch} MoS_2 FETs show a record high I_{ds} of 460 µA/µm at V_{ds} = 1.6 V, which is twice of the best reported I_{ds} on any TMD FETs. As a result, this technique is promising for realizing high-performance top-gate low-R_c MoS_2 FETs as well as other TMD based electronic devices.

References

[1] B. Radisavljevic *et al.*, *Nature Nanotechnology*, **6**, p. 147, 2011 [2] H. Wang, *et al.*, *IEDM*, P. 88, 2012 [3] Y. Yoon *et al.*, *Nano Letters*, **11**, p. 3768, 2011 [4] K. Majumdar *et al.*, *EDL*, **35**, p. 402, 2014 [5] H. Liu *et al., ACS Nano*, **8**, p. 1031, 2012 [6] S. Das *et al., Nano Letters*, **13**, p. 3396, 2013 [7] W. Liu, *et al.*, *IEDM*, p. 400, 2013 [8] Y.C. Du *et al., EDL*, **34**, p. 1328, 2013 [9] H. Fang *et al.*, *Nano Letters*, **12**, p. 3788, 2012 [10] H. Fang *et al.*, *Nano Letters*, **13**, p. 1991, 2013 [11] J. Chang, *et al.*, *arXiv: 1305.7162*, 2013 [12] Y.C. Du *et al., EDL* (in press), 2014 [13] J. Lee, *et al.*, *IEDM*, p. 491, 2013

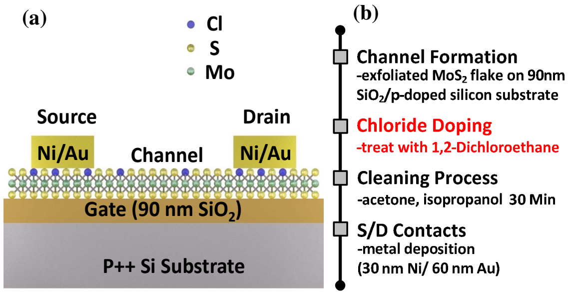

Fig. 1 (a) Schematic of the MoS_2 back-gate FET fabricated in this work. The gate dielectric is 90 nm SiO_2. The S/D contact metal is Ni (30 nm)/Au (60 nm). (b) Process flow for the MoS_2 back-gate FETs with the exfoliated MoS_2 flakes.

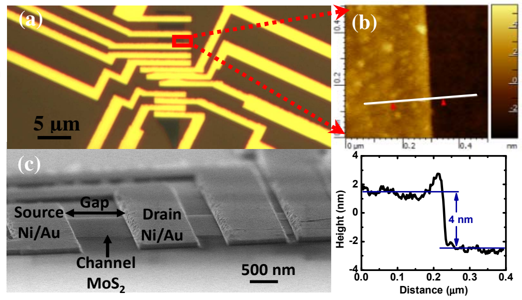

Fig. 2 (a) Optical image of the few-layer MoS_2 FETs with the Ni/Au contacts on 90 nm SiO_2/p^{++} Si substrate. (b) AFM image of a ~4 nm thick MoS_2 flake and the measured height at the flake edge. (c) SEM image of a MoS_2 TLM structure. The scale bar is 500 nm.

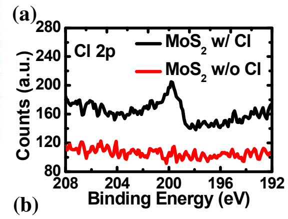

(b)

Cl isotope	SIMS count (a. u.) w/ Cl	SIMS count (a. u.) w/o Cl	Ratio
^{35}Cl	2451330	146257	16.76
^{37}Cl	750188	33215	22.59

Fig. 3 Cl signal from MoS_2 after the doping confirmed by (a) XPS and (b) SIMS.

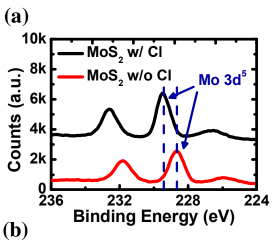

(b)

Peak	Binding energy (eV) w/o Cl	Binding energy (eV) w/ Cl	Shift (eV)
Mo $3d^5$	228.66	229.42	+ 0.76
S $2p^3$	161.39	162.22	+ 0.83

Fig. 4 (a) XPS spectra of Mo $3d^5$ w/ and w/o the Cl doping. A blue shift of 0.76 eV is observed. (b) Binding energy of the core levels w/ and w/o the Cl doping.

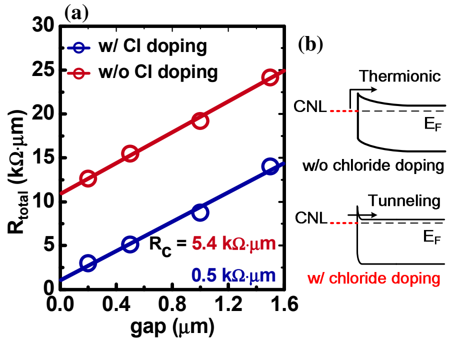

Fig. 5 (a) TLM resistances of MoS_2 FETs w/ and w/o the Cl doping at V_{bg} = 50 V. The R_c is reduced from 5.4 kΩ·µm to 0.5 kΩ·µm (b) Band diagram of the metal-MoS_2 contacts w/ and w/o the Cl doping. R_c is reduced due to the doping induced thinning of tunneling barrier width.

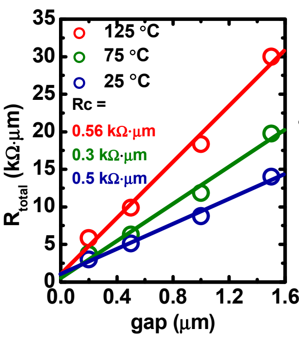

Fig. 6 TLM resistances of MoS_2 FETs at 25, 75, and 125 ºC. The extracted R_c remains similar from 25 ºC to 125 ºC, indicating the current is dominated by tunneling.

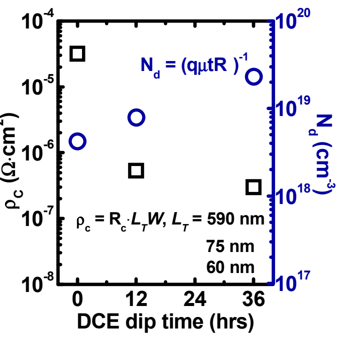

Fig. 7 DCE dip time dependence of ρ_c and N_d with the DCE treatment. The ρ_c is reduced by 100 after a 36 hours DCE treatment. N-type doping density of 2×10^{19} cm^{-3} is

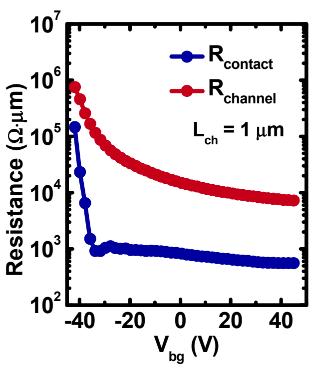

Fig. 8 $R_{channel}$ and $R_{contact}$ vs. V_{bg} for the 1 µm device. The $R_{contact}$ shows very weak dependence on the V_{bg} when V_{bg} > -30 V indicating heavily doped contact regions.

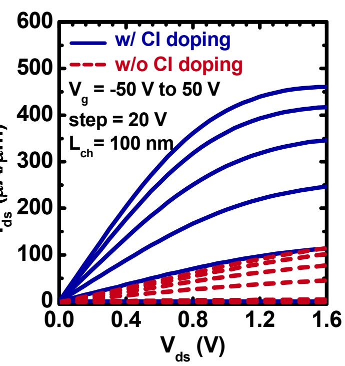

Fig. 9 Output characteristics of the 100 nm L_{ch} MoS_2 FETs w/ and w/o the Cl doping. A record high I_{ds} of 460 µA/µm is obtained.

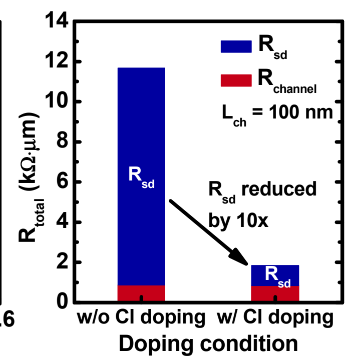

Fig. 10 Component of R_{total} for the two devices. The R_{total} of 100 nm L_{ch} MoS_2 FET is reduced from 11.7 kΩ·µm to 1.85 kΩ·µm due to the Cl doping.

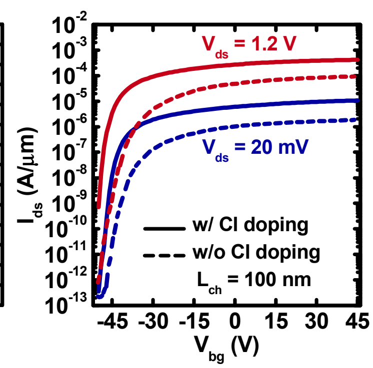

Fig. 11 Transfer characteristic curves of the 100 nm L_{ch} MoS_2 FETs w/ and w/o the Cl doping. The I_{on}/I_{off} ratio is 6.3×10^5 at V_{ds} = 1.2 V.

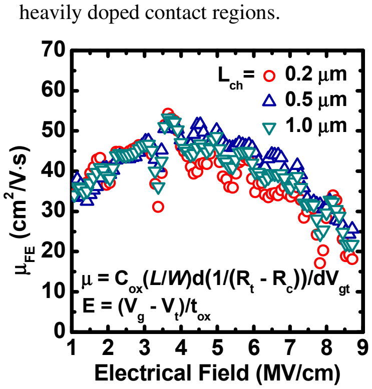

Fig. 12 Calculated intrinsic field-effect motilities as a function of the *gate field* for the MoS_2 FET with various L_{ch}.

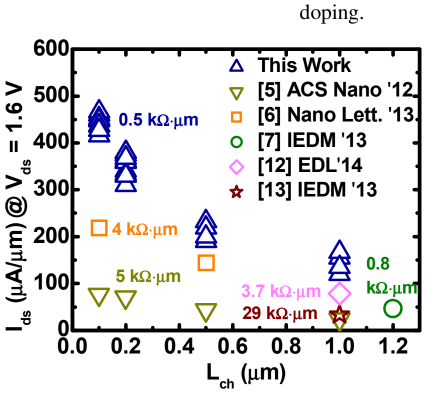

Fig. 13 Benchmarking of the I_{ds} @ V_{ds} = 1.6 V and the R_c in the reported MoS_2 back-gate FETs.

Summary of present work	
EOT	90 nm
L_{ch}	100 nm
R_c	0.5 kΩ·µm
ρ_c	3×10^{-7} Ω·cm²
I_{ds}	460 µA/µm @ 1.6 V
I_{on}/I_{off}	> 6.3×10^5 @ 1.2V
max. μ_{FE}	50-60 cm²/V·S

Table. 1 Summary of the electrical performance of the MoS_2 FETs in this work.

Acknowledgement:

The work at Purdue University is supported by SEMATECH and SRC. The authors would like to thank Hong Zhou, Yexin Deng and Zhe Luo for the valuable discussions and technical assistance.